ELSEVIER

Polymer 43 (2002) 831–838

polymer

www.elsevier.com/locate/polymer

A possible mechanism for cross-tie fibril generation in crazing of amorphous polymers

M.G.A. Tijssens[a,*], E. van der Giessen[b]

[a]*Delft University of Technology, Kluyverweg 1, 2629 HS, Delft, The Netherlands*
[b]*University of Groningen, Nijenborgh 4, 9747 AG, Groningen, The Netherlands*

Received 29 May 2001; accepted 6 September 2001

Abstract

A possible mechanism for cross-tie fibril generation in crazes of amorphous polymers is proposed. Detailed finite element calculations are performed on an axisymmetric model of a single fibril inside the craze. These calculations suggest that the hydrostatic stress inside the fibril is large enough to cause cavitation and subsequent growth of initial imperfections inside the fibril. The calculations demonstrate that these cavities will then grow by local plastic flow around them, leading to a continuous network of main fibrils interconnected by cross-tie fibrils.

Keywords: Amorphous polymers; Crazing; Cross-tie fibril

1. Introduction

The failure mechanisms in amorphous polymers can be roughly divided into shear yielding and crazing. The initiation of crazing is primarily controlled by the hydrostatic stress, whereas shear yielding is a result of large shear stresses. Shear yielding alone does not lead to fracture immediately but intersecting shear bands may assist in triggering crazing by locally enhancing the hydrostatic stress [1,2].

Based on microscopic observations, the internal structure of crazes is now generally assumed to be a structure of long 'main' fibrils, running from one craze–bulk interface to the opposite one, interconnected by cross-tie fibrils. The main fibrils are responsible for the extended load carrying capacity of crazes perpendicular to the orientation of the craze, whereas the cross-tie fibrils lend the craze some tangential load carrying capacity [3].

Although the breakdown of crazes can be triggered by the presence of dust inclusions [4], the cross-tie fibrils have recently been identified as playing an important role as well. Modeling the craze as an anisotropic continuum, Brown [3] showed that cross-tie fibrils are responsible for an increase in stress in the main fibrils large enough to cause failure of the backbone of the polymer molecules. Further detailed studies, with explicit modeling of the craze internal structure, were performed by Hui et al. [5] and Sha et al. [6]. These studies showed that the cross-tie fibrils are responsible for a further increase in stress in the main fibrils of roughly 20% as compared to Brown's model.

The importance of the cross-tie fibrils naturally leads to the question where they originate from. The propagation of the craze front is commonly considered (see e.g. Ref. [4]) as resulting either from a continuous generation of voids in front of a crack tip (for stress levels higher than, say, 0.4–0.5 times the yield stress) or from a meniscus instability mechanism. Argon and Salama [7] argued that through the meniscus instability mechanism, a craze structure evolves through which fluids can be freely transmitted, i.e. an 'open-cell' structure. They further argued that the repeated void nucleation process on the other hand results in a closed-cell structure. After the craze front has passed, the material inside the premature craze is stretched further and the polymer network eventually locks. Upon further widening, new polymer material is subsequently drawn into the craze [4], a process commonly called surface drawing. The voids generated by either the repeated void nucleation or meniscus instability mechanism are thus deformed to become highly prolate and the adjacent columns of material become the main fibrils. There seems to be no immediate mechanism by which cross-tie fibrils are generated that would interconnect these main fibrils.

To better understand the origin of cross-tie fibrils, we turn

* Corresponding author. Present address: Department of Aerospace Engineering and Mechanics, University of Minnesota, 107 Akerman Hall, 110 Union Street, S.E., Minneapolis, MN 55455, USA. Tel.: +1-612-625-6053; fax: +1-612-626-1558.
E-mail address: m.g.a.tijssens@lr.tudelft.nl (M.G.A. Tijssens).

0032-3861/02/$ - see front matter
PII: S0032-3861(01)00642-5

attention to a plane of isolated premature fibrils in the wake of a passing craze front which may either be the result of a repeated void nucleation process or a meniscus instability mechanism. In this configuration, we seek for a possible mechanism by which cross-tie fibrils may form. Our search is assisted by a finite element model that incorporates the growth of voids and fibrils by means of localized plastic flow. The complicated deformation history involving expansion of the void, interaction of shear bands, softening and re-hardening of the polymer material are accounted for in a material model that is described in Section 2. The numerical calculations discussed in Section 3 then hint at a possible, new mechanism of cross-tie fibril formation from cavitation inside primary fibrils.

2. Model of growing craze

We consider the widening of a craze, starting from premature fibrils in the wake of a passing craze front. We analyze how the fibrils grow and are in particular interested in the stress states inside the fibrils during growth. The objective is to suggest a novel possible mechanism for cross-tie fibril generation. For this, quantitative accuracy is not needed at this stage and therefore, we will make a number of simplifying assumptions that will render the analysis tractable. First of all, despite the fact that fibril diameters in amorphous polymers are typically on the order of tens of nanometers, we will be using a continuum description. Next, we approximate the distribution of premature fibrils by a hexagonal array of fibrils (Fig. 1a). The behavior of each fibril can then be represented with good accuracy by an axisymmetric cell containing a single fibril, see Fig. 1c. We further assume that the craze is symmetric with respect to the mid-plane of the craze. Such a craze fibril model is similar in spirit to those of Kramer and Berger [4] and of Leonov and Brown [8].

Taking advantage of the symmetry of the craze, widening is simulated by fixing the mid-plane and displacing the bulk material at some distance above the voids at a constant velocity $\dot{\delta}_n$. The stress or deformation state in the plane of the craze is generally unknown. We simply assume that the in-plane displacements are much smaller than those due to fibril growth, which means that the circumference of the cell cannot move in horizontal direction. Using the material model to be outlined below, the analysis of this problem is done by means of a finite element method that captures the very large strains that develop inside the fibril. The finite element mesh is shown in Fig. 1c.

We focus on amorphous polymers and assume that

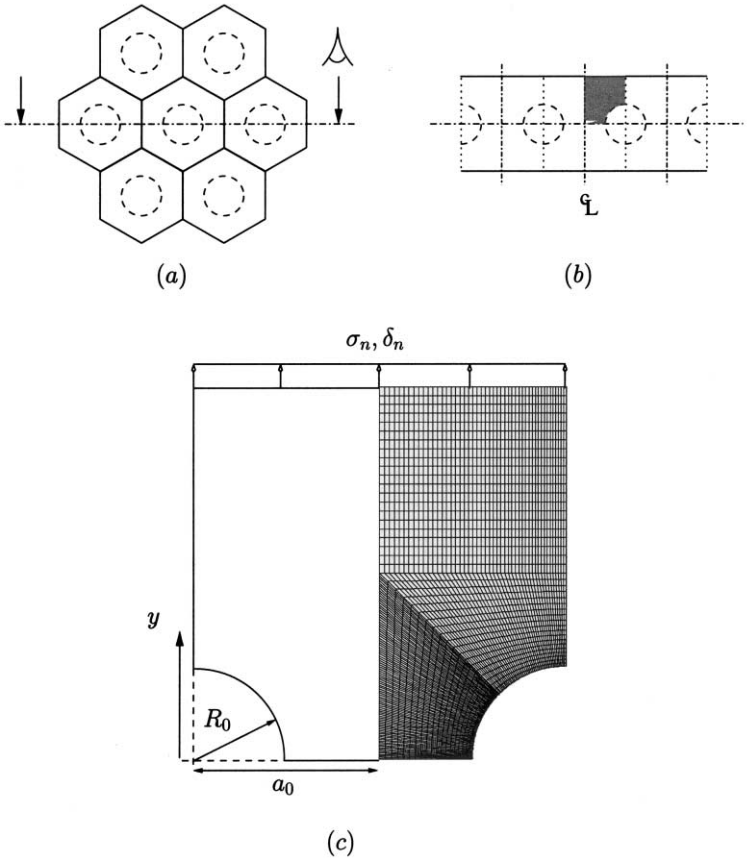

Fig. 1. (a) Idealized distribution of premature fibrils surrounded by toroidal voids in the wake of the craze front represented by (b) an axisymmetric cell containing a single fibril. Dimensions and finite element mesh are shown in (c).

around individual fibrils, the same deformation mechanisms are operating as during shear yielding of the glassy material at the macroscopic level. Thus, we can adopt the constitutive equations for large strain plastic flow based on original ideas by Boyce et al. [9] but with some modifications introduced later by Wu and Van der Giessen [10]. The actual form adopted here, along with a convenient numerical integration scheme, is given in Ref. [11]. For further details, one is referred to these references and the review in Ref. [12].

The material model has been explicitly developed for amorphous polymers and accounts for rate-dependent yielding, intrinsic softening and subsequent re-hardening. The rate of deformation is decomposed in an elastic and a plastic part. The elastic response is taken to be isotropic with Young's modulus E and Poisson's ratio ν.

Plastic flow is controlled by the driving stress $\bar{\sigma}_{ij}$ $(i,j \in 1,2,3)$ which is the difference of the actual stress σ_{ij} and a back stress b_{ij}. The back stress describes the hardening during continued plastic straining due to stretching of the polymer network. Its constitutive behavior is borrowed from the elasticity of rubber networks. Based on the work in Ref. [10], the principal components of the back stress, b_i, depend on the plastic stretches λ_i through a linear combination of the classical three-chain network description and the eight-chain network description given in Ref. [13]. The principal back stresses become unbounded when the plastic stretches λ_i approach the limit stretch $\lambda_{\max} = \sqrt{N}$ where N is a statistical network parameter. When this occurs, the network locks and further plastic flow is prevented. The second material parameter is the initial hardening modulus C^{R}.

Plastic flow by shear yielding is controlled by the equivalent shear stress $\tau = \sqrt{(1/2)\bar{\sigma}'_{ij}\bar{\sigma}'_{ij}}$ (sum on repeated indices). Here, $\bar{\sigma}'_{ij} = \bar{\sigma}_{ij} - \sigma_m\delta_{ij}$ is the deviatoric part of the driving stress, with $\sigma_m = (1/3)\bar{\sigma}_{kk}$ being the hydrostatic stress (δ_{ij} is the Kronecker delta). The magnitude of the plastic part of the rate of deformation is taken to be given by the expression for the plastic shear rate $\dot{\gamma}^{\mathrm{p}}$ in terms of the equivalent driving stress τ as given by Argon [14]:

$$\dot{\gamma}^{\mathrm{p}} = \dot{\gamma}_0 \exp\left[-\frac{As_0}{T}\left(1 - \left(\frac{\tau}{s_0}\right)^{5/6}\right)\right], \tag{1}$$

where $\dot{\gamma}_0$ and A are material parameters and T is absolute temperature. In order to account for pressure dependence, the athermal shear strength s_0 is taken as a linear combination of the hydrostatic stress σ_m and the shear strength s, $s_0 = s - \alpha\sigma_m$. Softening upon yield is incorporated by letting s evolve during plastic flow at a rate depending on the softening parameter h until it saturates at a value s_{ss}.

The plastic dissipation rate (per unit volume) during plastic flow is $\dot{D} = \tau\dot{\gamma}^{\mathrm{p}}$. The associated temperature rise can only be neglected if the generated heat quickly diffuses away from the fibril. From a one-dimensional argument, the importance of conductivity in a particular situation can be assessed by the non-dimensional parameter κ defined as

$$\kappa = \frac{kt_0}{\rho_0 c_{\mathrm{v}} L_0^2}, \tag{2}$$

where k is the thermal conductivity, ρ_0 is the density, c_{v} is the heat capacity, t_0 is a characteristic time scale and L_0 a characteristic length scale associated with the problem. For $\kappa \gg 1$, isothermal conditions prevail, while $\kappa \ll 1$ corresponds to adiabatic conditions. For polycarbonate, the values are $k = 0.2$ W/mK, $\rho_0 = 1200$ kg/m^3, $c_{\mathrm{v}} = 1200$ J/kg K. The radius of the initial void R_0 is taken as the characteristic length L_0 and equals 10 nm. The drawing rate $\dot{\delta}_n$ that is used in the calculations results in a time scale of the process of roughly 1 s. The value of κ therefore equals approximately 10^9, showing that fibril drawing is an isothermal process and temperature changes do not need to be accounted for.

3. Numerical analysis of fibril drawing process

The initial condition is that of an isolated premature fibril surrounded by a toroidal hole. In the first calculations, we will completely ignore the local deformations that led to this stage and assume that all material is in its virgin state. The material parameters mentioned in Section 2 are taken to be representative for polycarbonate, i.e. $E = 910$ MPa, $\nu = 0.3$, $s_0 = 97$ MPa, $s_{\mathrm{ss}} = 77$ MPa, $\dot{\gamma}_0 = 2.0 \times 10^{15}$ s^{-1}, $h = 500$ MPa, $\alpha = 0.08$, $A = 240$ K/MPa, $N = 12$, $C^{\mathrm{R}} = 4$ MPa. The temperature is taken to be $T = 294$ K. We assume that the craze widens at a rate of $\dot{\delta}_n = 10$ nm/s; changing this rate by a factor of ten changes the resulting stresses only by a few percent. Because of the absence of material length scales in this type of analysis, the geometry enters the results only through the ratio a_0/R_0, where a_0 is half the fibril spacing; a value of $a_0/R_0 = 2$ seems realistic. The results will be presented in normalized form, e.g. the normalized stresses σ_{ij}/s_0 will depend only on the dimensionless parameters $\dot{\gamma}_0/(\dot{\delta}_n/R_0)$, E/s_0, ν, s_{ss}/s_0, h/s_0, α, As_0/T, N and C^{R}/s_0.

The three snapshots in Fig. 2 demonstrate how a premature fibril grows from its initial state to an elongated fibril (the hydrostatic stress distributions will be discussed shortly). Early in the growth process, the intrinsic softening of the material after yield gives rise to shear bands emanating from the outside of the fibril along the center plane, Fig. 3. These strongly localized shear bands propagate through the premature fibril and hit the centerline of the axisymmetric cell. At that moment, the fibril begins to contract and the overall craze normal stress continues to decrease strongly, see Fig. 4. Upon further widening, the shear bands propagate towards the bulk side of the material (see the deformed shapes in Fig. 2) due to the re-hardening of the material. Extension of the fibril thus is due to the shear band propagation, which in the last stage shown in Fig. 2 transports material from almost above the original void into the fibril. Inside the fibril, the material is highly stretched in the loading direction, and is in fact locked to prevent further flow.

Fig. 5 shows the radial stress component (i.e. in the plane

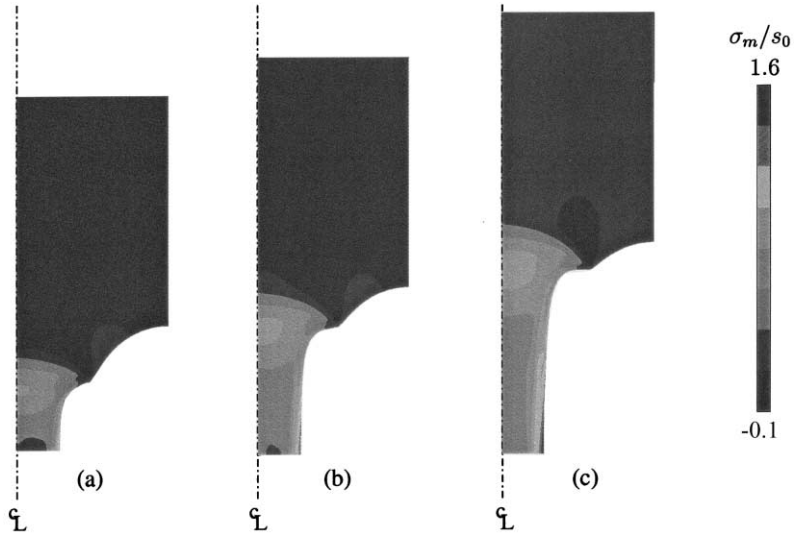

Fig. 2. Hydrostatic stress distribution for a single, axisymmetric fibril without imperfections for increasing applied vertical displacement at the top of the fibril (also see Fig. 4).

of the craze) along the ligament between neighboring fibrils at the same moment as in Fig. 2c. A tensile stress has gradually developed above the dome between fibrils. The peak value of approximately 20 MPa at this stage will grow even larger upon further growth, and will enhance disentanglement and may eventually become large enough to cause scission of molecules. Disentanglement and chain scission may cause failure in this region to accommodate further widening of the craze [4]. It is interesting to note that Fig. 5 also shows that this radial stress along the centerline of the fibril can attain even higher values locally. The location of the stress peak roughly coincides with the location where the current shear band hits the centerline.

Of more interest for the present purpose is the distribution of hydrostatic stress σ_m inside the fibril, which is shown in Fig. 2. From this figure, it is seen that the hydrostatic stress attains a local maximum over the regime in which the shear is currently most active. The distribution along the center of the fibril, shown in Fig. 6, more clearly reveals that not only there is a clear peak but that its magnitude increases as the drawing process continues. The values found in this analysis are on the order of $\sigma_m/s_0 = 0.6$–1.0. According to the analysis given by Steenbrink and Van der Giessen [15], a cavitation instability can occur in polymers with the same constitutive behavior as considered here, for hydrostatic stresses as low as $\sigma_m/s_0 = 0.7$. Strictly speaking, such a cavitation instability is the spontaneous nucleation of a void inside an otherwise homogeneous material; an alternative but practically equivalent view is that of the unstable growth of a void from a pre-existing flaw or even inhomogeneity. It is fully similar to the concept of cavitation in rubbers as explored by Gent [16], but now occurs in a plastically flowing material. Leaving aside the details, the important observation is that the hydrostatic stresses inside a fibril can become high enough for a cavitation instability to occur.

4. From cavitation to cross-tie fibrils

The analysis in Ref. [15] applies to the material in the undeformed, hence isotropic state and subjected to pure hydrostatic expansion. Neither one of these presumptions strictly applies to the material inside the fibril. In this section, we present the results of similar calculations but assume the presence of an imperfection in the form of a

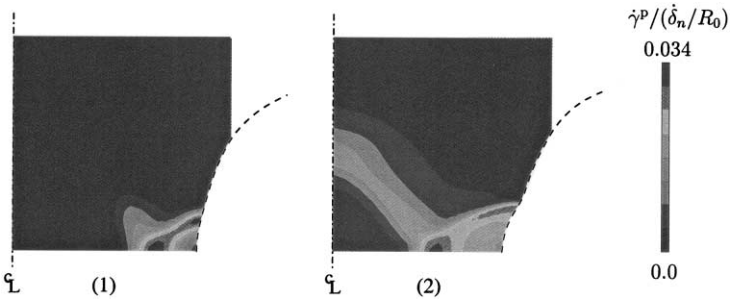

Fig. 3. Contours of the normalized plastic shear rate $\dot{\gamma}^p$ just before global localization of deformation occurs (also see Fig. 4).

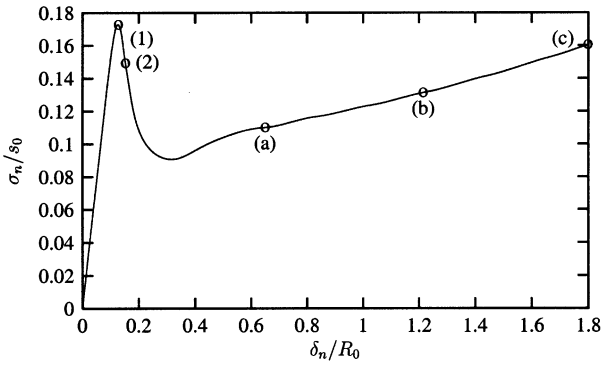

Fig. 4. Stress–strain curve for the perfect fibril in which the points (a)–(c) and (1)–(2) correspond to the instants shown in Figs. 2 and 3, respectively.

very small, spherical void along the centerline (initial radius $r_0 = 0.01R_0$, i.e. on the order of 0.1 nm). The calculation will then show if this void grows substantially (as the cavitation instability analysis would suggest) or that it does not.

We first choose a rather arbitrary position for the imperfection of $y/R_0 = 0.7$. At this position, the previous analysis predicts a hydrostatic stress peak of around $0.85s_0$ when δ_n is around $1.6R_0$. The evolution of the cross-sectional area (as a convenient measure of size, illustrated in Fig. 7) of the tiny void at this position with increasing craze opening δ_n/R_0 is shown in Fig. 8. First, the void size increases slightly due to elastic deformation which is followed by a sudden rapid increase favored by very local shear bands around the imperfection. The growth comes to a rest once the fibril starts to neck down and the toroidal hole expands. However, for increasing deformation, we see that the rate at which the imperfection grows, increases again and increases to do so. This unstable growth happens clearly at a much earlier stage, $\delta_n/R_0 \approx 0.5$, than expected from the previous analysis. This indicates that the hydrostatic stress in this case does not even have to reach values of $0.85s_0$ for an initial, very small void to expand rapidly. At the end of the calculation shown in Fig. 8, where the area increase is roughly a factor of 5, the volume has increased by a factor of about $5^{3/2} \approx 11$.

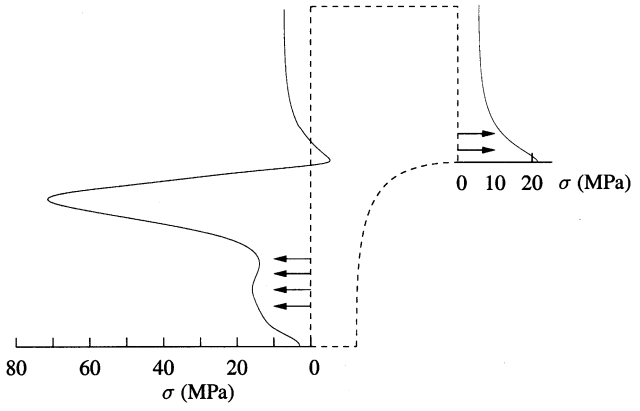

Fig. 5. Radial stress component on the edges of the cell at $\delta_n/R_0 = 1.8$.

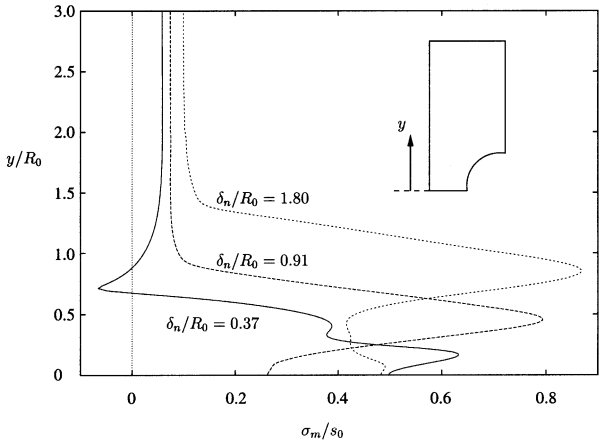

Fig. 6. Hydrostatic stress along the centerline of the fibril.

The calculation shown in Fig. 8 was stopped because of excessive distortion of the finite element mesh around the small void. We do expect however that the void will actually continue to grow further. Now, if this void has grown to a size equal to a sphere of radius R_0, we have to remember that there is another, similar void in the neighboring fibrils. In the cross-sectional view of Fig. 9, this suggests that the ligament in between these two voids serves as another fibril that grows while these voids expand. As this proceeds, one can imagine that new voids nucleate by cavitation instability. As this process continues, a network of fibrils and voids develops. The cross-tie fibrils in this picture thus evolve due to repeated void nucleation and growth in existing fibrils, as illustrated in Fig. 9. Evidently, we have taken here a two-dimensional view. In three dimensions, a void inside a fibril does not lead to two fibrils as in the two-dimensional picture. However, the void will not nucleate exactly in the center, and the symmetry is broken. What will happen subsequently is not clear, but it is not ruled out that the nucleated void coalesces with the toroidal hole and that an interconnected network of fibrils evolves. The key element of this mechanism remains the nucleation of

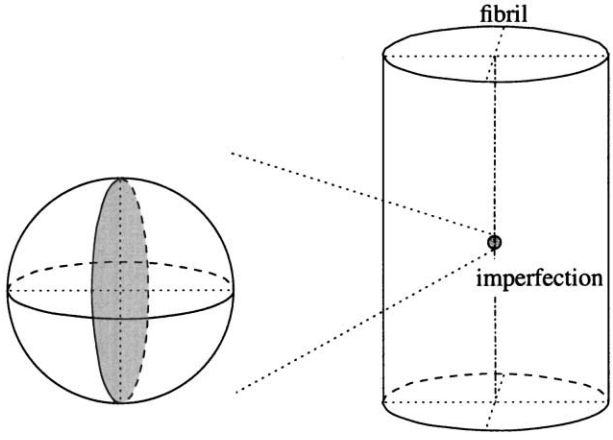

Fig. 7. Illustration of the cross-sectional area A_0 of the imperfection used as a convenient measure of size.

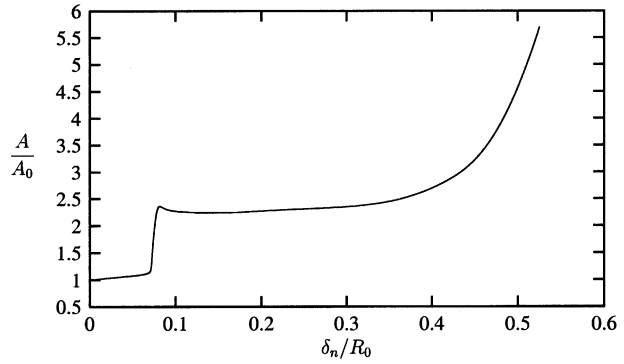

Fig. 8. Evolution of the area of the imperfection with increasing load. First, the imperfection grows rapidly, but this stops due to expansion of the toroidal hole. Later, the imperfection continues to grow.

voids inside the propagating shear bands that draw the existing fibrils.

5. Refinements

The foregoing calculations are idealized in several ways, including the assumptions that the imperfections are spherical voids and that the material is in its virgin state. In addition, we have assumed an imperfection at an arbitrary location. To explore the consequences of these assumptions, we examine two situations, one in which the imperfections are elongated and the material is virgin initially, and another one in which the imperfections are spherical initially, but the material is rejuvenated. In each of these, we ask if there is a critical position of the imperfection for which cavitation is most easy.

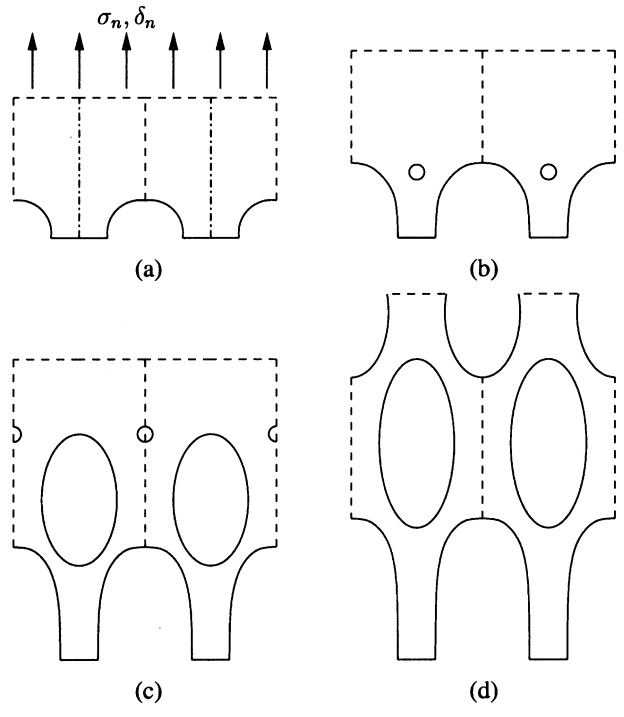

Fig. 9. Illustration of the proposed mechanism: (a) the premature craze is loaded, widens, and (b) a cavitation instability occurs inside the fibrils. (c) The voids grow and another cavitation instability develops in between them. The mechanism repeats itself (d) resulting in a cross-tie fibrillar network.

5.1. Elongated imperfections and virgin material

As mentioned before, the material inside the fibril in our starting configuration will have undergone deformation already during the nucleation of the craze, mostly stretching in the fibril direction. As a consequence, any defect in the material that is, say, spherical before crazing will have been stretched already when it is in our starting configuration. Here, we examine the effect of elongation of imperfections. We roughly estimate the stretch of the material in the fibril and use this to modify the shape of the imperfection.

The stretch of the material inside the fibril is calculated from the assumption that there is no volume change when the material in the fibril contracts horizontally as the fibril is nucleated. As illustrated in Fig. 10, this means that the initial volume $\pi(2R_0)^2 dy_0$ of an element is equal to that after the formation of the fibril, $\pi r^2(y)dy$, with $r(y) = 2R_0 - \sqrt{R_0^2 - y^2}$. This results in

$$dy/dy_0 = \left[\frac{5}{4} - \frac{1}{4}(y/R_0)^2 - \sqrt{1-(y/R_0)^2}\right]^{-1}, \qquad (3)$$

which equals the vertical stretch λ. This formula yields a stretch of $\lambda = 4$ for $y = 0$ and no elongation ($\lambda = 1$) for $y = R_0$. The assumption of no volume change implies that the circumferential stretch equals $\sqrt{1/\lambda}$. However, since the imperfections are already of molecular size, we will not account for this reduction of size in circumferential size. Hence, the stretch according to Eq. (3) is taken to effect only the vertical dimension of the imperfection.

The results for the growth of the imperfection for increasing vertical offset from the horizontal symmetry plane are given in Fig. 11. The growth curve for each case is essentially similar to that in Fig. 8, thus indicating that the initial void shape is not very important. Also from these analyses, and others that we have performed with material parameters for virgin material, it is clear that the imperfection that is closest to the horizontal symmetry plane will

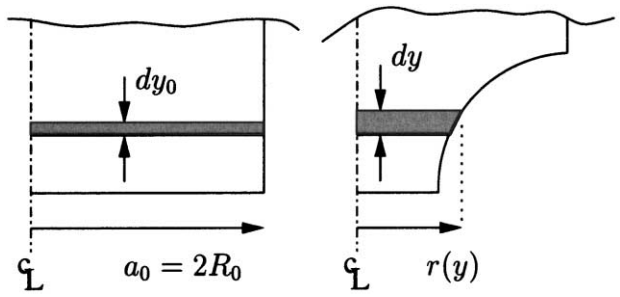

Fig. 10. Illustration of how the stretch in the material of the fibril is estimated from the assumption of zero volume change.

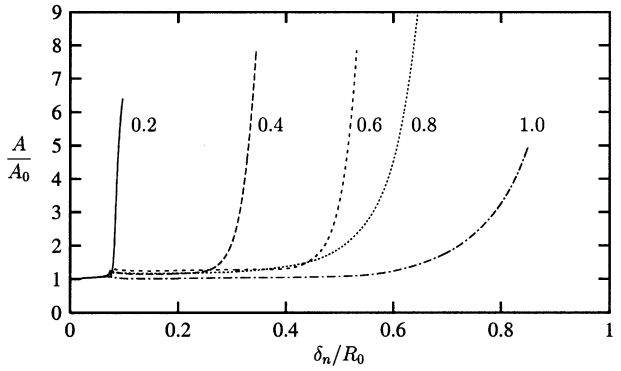

Fig. 11. Evolution of the area of elongated imperfections with increasing load. The vertical position y/R_0 of the imperfection is indicated in the figure.

grow first. Apparently, the hydrostatic stress is already high enough there for the void to expand, even though according to Fig. 6, higher stress peaks occur (at later stages) further away from the symmetry plane.

5.2. Rejuvenated material

In the second set of calculations, we assume that during the nucleation of the craze, all material situated in $0 < y < R_0$ has yielded. This is motivated by the calculations for the perfect fibril, where we have seen that expansion of the toroidal hole takes place by shear bands propagating upwards and stretching the material inside the fibril, see e.g. in Fig. 3. We imagine a similar process to occur during the formation of the fibril and the toroidal hole. As a consequence, it is likely that the material inside the premature fibril will not exhibit any intrinsic softening anymore once the craze front has passed: the material is rejuvenated. For simplicity, we take all material for $0 < y < R_0$ in the fibril to behave as elastoplastic without softening, as illustrated in Fig. 12. The imperfections assumed inside the fibril are taken to be spherical initially, based on the results in Section 5.1.

The results for the growth of the imperfections is given in Fig. 13. We see that if the imperfection is located further

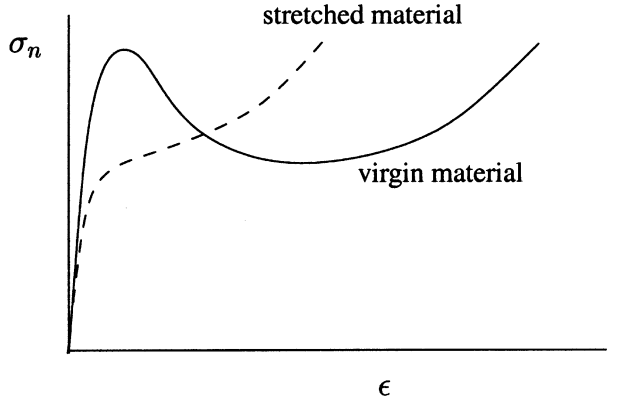

Fig. 12. Schematic of the uniaxial stress-strain behavior of the stretched material relative to the virgin material.

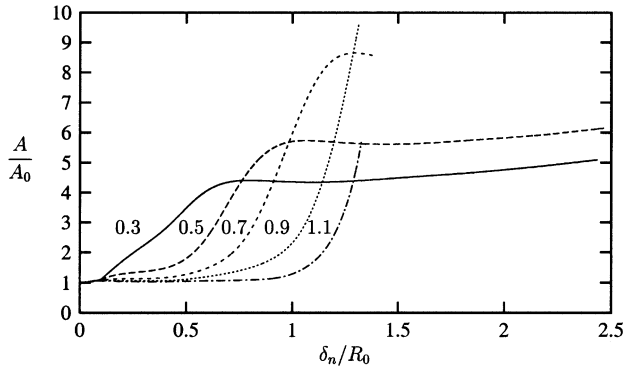

Fig. 13. Evolution of the area of spherical imperfections in which the lower part of the fibril material consists of elastoplastic material without intrinsic softening. The vertical position y/R_0 of the imperfection is indicated in the figure.

away from the horizontal symmetry plane, the void tends to grow later, but it also tends to expand further. Contrary to the virgin material, the rejuvenated material does not display a strongly localized shear band. The stresses inside the fibril are more evenly distributed as it contracts. Now that the entire fibril is an area of less intense deformation, the imperfections that are close to the symmetry plane do expand, but the expansion quickly comes to a rest as the deformation continues to travel upwards along the fibril. It was shown in Fig. 6 that the hydrostatic stress near the center of the fibril reaches a peak value which increases with increasing distance from the symmetry plane. This makes imperfections further away from the horizontal symmetry plane a more likely candidate for continued expansion.

6. Conclusion

A possible mechanism for cross-tie fibril generation inside crazes in amorphous polymers is proposed. Finite element calculations based on an axisymmetric representation of the premature fibril structure behind the craze front are used to motivate that cross-tie fibrils are generated inside the fibrils by initiation and growth of voids. A network of cross-tie fibrils results when this mechanism is repeated upon further drawing of the polymer material.

There are a number of limitations and objections that can be raised, among which are the limitations of the continuum material model and the simplification to an axisymmetric analysis. To further analyze the possibility of the proposed mechanism, one should extend the material model to include disentanglement and scission of the polymer network [4]. However, the incorporation of these into the material model is not clear at this stage. The axisymmetry excludes the actual formation of a three-dimensional network of fibrils, as discussed in Section 4. Fully three-dimensional analyses would be necessary to examine this in detail.

References

[1] Yamamoto T, Furukawa H. Polymer 1995;36:2393.
[2] Lai J, Van der Giessen E. Mech Mater 1997;25:183.
[3] Brown HR. Macromolecules 1991;24:2752.
[4] Kramer EJ, Berger LL. Adv Polym Sci 1990;91/92:1.
[5] Hui CY, Ruina A, Creton C, Kramer EJ. Macromolecules 1992;25:3948.
[6] Sha Y, Hui CY, Ruina A, Kramer EJ. Acta Mater 1997;45:3555.
[7] Argon AS, Salama MM. Philos Mag 1977;36:1217.
[8] Leonov AI, Brown HR. J Polym Sci 1992;29:197.
[9] Boyce MC, Parks DM, Argon AS. Mech Mater 1988;7:15.
[10] Wu PD, Van der Giessen E. J Mech Phys Solids 1993;41:427.
[11] Wu PD, Van der Giessen E. Eur J Mech A/Solids 1996;15:799.
[12] Van der Giessen E. Eur J Mech A/Solids 1997;16:87.
[13] Arruda EM, Boyce MC. J Mech Phys Solids 1993;41:389.
[14] Argon AS. Philos Mag 1973;28:839.
[15] Steenbrink AC, Van der Giessen E. Int J Damage Mech 1997;6:317.
[16] Gent AN, Lindley PB. Proc R Soc Lond A 1958;249:195.